

# The Mechanical Characteristics of Human Endothelial Cells in Response to Single Ionizing Radiation Doses By Using Micropipette Aspiration Technique

Alireza Mohammadkarim<sup>1</sup>, Manijhe Mokhtari-Dizaji<sup>2,\*</sup>, Ali Kazemian<sup>3</sup>, Hazhir Saberi<sup>4</sup>,  
Mohammad Mehdi Khani<sup>5</sup> and Mohsen Bakhshandeh<sup>6</sup>

<sup>1</sup>Department of Medical Physics, Faculty of Medical Sciences, Tarbiat Modares University, Tehran, Iran and Faculty of Medicine, Semnan University of Medical Sciences, Semnan, Iran.

<sup>2</sup>Department of Medical Physics, Faculty of Medical Sciences, Tarbiat Modares University, Tehran, Iran.

<sup>3</sup>Radiation Oncology Research Center, Cancer Institute, Tehran University of Medical Sciences, Tehran, Iran.

<sup>4</sup>Department of Radiology, Imam Khomeini Hospital, Tehran University of Medical Sciences, Tehran, Iran.

<sup>5</sup>Department of Tissue Engineering and Regenerative Medicine, School of Advanced Technologies in Medicine, Shahid Beheshti University of Medical Sciences, Tehran, Iran.

<sup>6</sup>Radiology Technology Department, Faculty of Paramedical Sciences, Shahid Beheshti University of Medical Sciences, Tehran, Iran.

\*Corresponding Author: M. Mokhtari-Dizaji. Email: mokhtarm@modares.ac.ir.

**Abstract:** The mechanical properties of living cells are known to be promising biomarkers when investigating the health and functions of the human body. Ionizing irradiation results in vascular injury due to endothelial damage. Thus, the current study objective was to evaluate the influence of continuous radiation doses on the mechanical properties of human umbilical vein endothelial cells (HUVECs), and to identify Young's modulus (E) and viscoelastic behavior. Single-dose (0, 2, 4, 6, and 8 Gy) radiation was applied to HUVECs using a Cobalt-60 treatment machine in the current vitro irradiation study. Thereafter, a micropipette-aspiration technique was used to measure the elastic modulus of the HUVECs in control and radiation-induced samples. Confocal imaging was then performed for following of the cytoskeletal reorganization of the HUVECs in response to the different radiation doses. Significant enhanced adhesion of the elastic modulus of the HUVECs was observed. The dose value was seen to increase from 0 Gy to 8 Gy. A linear relationship was observed between the 0 Gy and 8 Gy doses following an examination of the dose-response curve for elastic modulus after irradiation. The correlation coefficient was found to be 0.955 and the sensitivity of the dose-elastic modulus to be 7.69 Pa.Gy<sup>-1</sup> following analysis of the linear portion of the response curve. Also, a significant increment in stiffness accompanied with the considerable drop in creep compliance curve was detected in radiation-induced groups. Biomechanics-based analysis can provide a platform from which to assess the response of the endothelium to radiation when studying vascular system behavior during the cancer therapy process.

**Keywords:** Endothelial cells; ionizing radiation; micropipette aspiration; elastic modulus; cytoskeletal remodeling

## 1 Introduction

The “vascular endothelium” is a thin monolayer of cells that acts as an interface between the interior surface of the vascular system and blood within the vessel. The endothelium is known to be a highly dynamic organ system that provides a barrier to the blood-vessel wall mass transportation of materials. The endothelial layer also responds to changes in the extracellular environment in order to preserve normal vascular system functioning [1-3]. The growth and behavior of the endothelium is strongly

influenced by the mechanical properties of the endothelial cells [4]. The endothelial cells are known to produce various kinds of cytokines and vasoactive compounds, including endothelium-derived relaxing factor, endothelium-derived contractile factors, and prostacyclin; the latter which controls vascular tone, the internal diameter of the vessels, and blood flow. The mechanical behavior of the endothelial cells is also closely related to blood-vascular wall mass transport phenomena [5,6]. Bischof et al. [7,8] described how the mechanical properties of cells are affected by their physiological activity, including motility, proliferation, adhesion, and differentiation. It was demonstrated in previous studies that the mechanical properties of endothelial cells are dependent on environmental and chemical stimuli [5,6].

Damage to the normal tissue surrounding the tumor, including the large vessels, is a major limiting factor of radiation therapy treatment [9]. The radiobiological effects of ionizing radiation, such as atherosclerosis, radiation-induced stenosis, vascular blowout, and incensement of the common carotid intima-media thickness of the vessel wall, have been reported *in vivo* studies [10-12].

Vascular injuries are known to be the result of an increase in the permeability of the endothelial cells. Monocytes differentiate into macrophages in the vessel wall. Oxidized low-density lipoproteins in the endothelial cells are scavenged and passed into the sub-endothelial area where bottom cells are formed. Platelets collect at the injury space and release different growth factors that cause the smooth muscle cells to migrate to the interface between the vessel wall and the blood. Deposition of the extracellular matrix leads to vascular injuries [12-14].

Recently, the focus in many studies has been on determining how vessel endothelial cells respond to ionizing radiation as the cells at risk in diverse biological models [9,15-19]. Previously, it has been described that fractionated radiotherapy affects the mechanical behavior of endothelial cells [20]. Moreover, it has been proved that differences in the elastic parameter of endothelial cells provide a quantitative description of radiobiological effects for assessing the dose-response relationship in the linear region of the sigmoid curve as a biological dosimetry procedure in fractionated radiotherapy [21]. In stereotactic radiotherapy methods that known as the modern radiotherapy procedures, a high dose fraction is used to treat the lesions [22]. To the best of our knowledge, a comparison of the mechanical properties of endothelial cells after single exposure with those of non-irradiated cells as a biological dosimeter has not been evaluated in any study to date.

Zheng et al. [23] utilized atomic force microscopy (AFM) to investigate the stiffness of tongue squamous cell carcinoma (TSSC) in response to ionizing radiation doses. It was demonstrated that the Young's modulus of irradiated TSSC decreased with increasing dose exposure (from 0 Gy to 4 Gy) and was associated with a decrease in the signal intensity of stained F-actin fibers. AFM is often employed to assess the elastic behavior of materials [24-28]. It has been proposed as the most suitable method for the accurate localized measurement of cell elasticity [14,19]. Beside AFM, micropipette aspiration (MA) is usually utilized to assess the mechanical characterization of cells, including the elastic and viscoelastic properties of individual living cells [6,29-31]. As opposed to AFM, suitable for measuring the local properties of a cell, the use of MA is more appropriate when evaluating the whole biomechanical properties of a living cell [6]. Compared to AFM, MA seems to be a more valuable technique to characterize the capability of a cell to flow in response to an instantaneous application of constant pressure and to compare the creep behavior of the cells among the treatments [32].

Thus, the objective of the current study was to investigate the effects of ionizing irradiation on the elastic modulus and the time-dependent mechanical behavior of endothelial cells using MA. The efficiency of this method and the sensitivity of the endothelial cells were determined for a range of absorbed doses through the examination of the dose-response curve of the elastic modulus. Moreover, the alterations of the creep compliance curve in response to different ionizing doses were quantified by using the standard three-element linear viscoelastic solid model. Cytoskeletal remodeling of the endothelial cells in response to different ionizing doses, as a main contributor to the cellular adaptive reaction to environmental stimuli, was also performed using confocal microscopy imaging.

## 2 Materials and Methods

Human umbilical vein endothelial cells (HUVECs) acquired from the National Cell Bank of Iran at the Pasteur Institute of Iran, Tehran, Iran, were cultured in a T-flask in Dulbecco's Modified Eagle Medium: Nutrient Mixture F-12-containing medium (1:1) supplemented with 10% fetal bovine serum (FBS) and 1% penicillin-streptomycin (Sigma-Aldrich, Germany). The cells were kept in a humidified incubator at 37°C with 5% CO<sub>2</sub>. The cell culture medium was changed twice weekly. The HUVECs used in the radiobiological experiments were between passages 4 and 7. In the last passage stage, the cells were prepared in 6-well tissue culture plates (Sigma, Germany) for the irradiation process, actin cytoskeleton staining, and MA.

The cells grown in the 6-well plates were irradiated with 1.25 MeV of energy, using a Cobalt-60 machine (Cobalt teletherapy unit, Theratron 780 C, AECL, Ottawa, Canada). The cells for each individual dose were irradiated according to the absorbed dose range of 0-8 Gy in 2 Gy steps. Cell irradiation was performed in a vertical direction, taking into account the required build-up thickness of the culture medium at room temperature in the absence of CO<sub>2</sub>. The non-irradiated cells (0 Gy) were considered to be the control group. In the preparation stages, 3 cm of polystyrene phantom was placed beneath the dishes to prevent backscatter radiation. Irradiation was performed at constant conditions [a field size of 30 × 30 cm<sup>2</sup>, a source surface distance of 80 cm, and a build-up depth of 0.5 cm (dmax)]. Thereafter, the radiation-induced HUVECs were incubated at 37°C and experimental investigations were performed for 24 hours following irradiation.

Visualization of the cytoskeleton of the HUVECs was performed with confocal microscopy using a Leica TCS SP5 Confocal® microscope (Leica Microsystems, Buffalo Grove, USA). The coverslips were placed over the well to perform confocal imaging of each group. The cells seeded therein were prepared using a protocol which was similar to that adapted for the radiobiological studies that were described in previous work [16]. Prior to confocal imaging, the cells placed on the coverslips were washed three times with phosphate-buffered saline. The actin filaments were labeled for an hour at room temperature using Alexa Fluor® 488 Phalloidin® (Thermo Fisher Scientific Waltham, USA). Then, the perimeter around the multiple cells membrane of each group was counterered with Image J software for assessing the cell area and cell perimeter. Observation of the nuclei structure of the cells was carried out using DAPI® (4',6-diamidino-2-phenylindole) staining (Thermo Fisher Scientific) and imaging with a fluorescent microscope (100 × magnification), as described in previous study [2]. Then, the area and perimeter of nuclei were quantified in multiple cells of each group by counterering the nuclear body with Image J software. In the next step, shape index of each subject was defined as  $(4\pi \times \text{cell area}) / (\text{cell perimeter})$ . As the shape index approaches 0, the subject assumes a linear, elongated morphology. As the shape index approaches 1, the subject spreads out and becomes more circular [33].

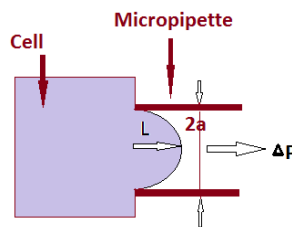


**Figure 1:** A schematic depiction of micropipette aspiration, showing how a suspended cell was aspirated in the micropipette needle following the exertion of specific negative suction pressure during monitoring of the cell aspiration process ( $\Delta P$ : negative pressure, L: aspirated length of the cell)

The advantages and disadvantages of measuring single-cell mechanical properties using MA have previously been discussed [6,29]. With MA, the biomechanical properties of a cell are measured with high reproducibility. Briefly, micropipette needles with an internal diameter ranging from 5.5-10.0  $\mu\text{m}$  were used to perform the aspiration tests for cells with various sizes. Before each experiment, the micropipettes were

coated with Sigmacote®, a siliconizing reagent (Sigma-Aldrich, Germany), to prevent adhesion of the HUVECs to the inner wall of the needle. It should be noted that based on the Maxwell model, the diameter of selected cell was greater than  $2.5 \times$  internal diameter of micropipette. Thereafter, the cells were detached from their substrate using trypsinization in  $\geq 4$  minutes to avoid cell disruption and thrombosis formation which might have affected the biomechanical properties of the cells at room temperature. A suspended cell was aspirated in the micropipette needle through the exertion of specific negative suction pressure for each experiment. The cell aspiration process was monitored continuously (Fig. 1).

Aspiration of the cells during the elastic behavior determination process was recorded using a video camera and the aspiration length of each cell was measured using AxioVision® software 4:8. Prior to each aspiration, an equilibrium pressure of 10 Pa was applied to the suspended cells for 60 s to allow them to reach a stable condition. Once equilibrium had been achieved, increasing negative pressure (60-520 Pa) was exerted on five occasions on the aspirated samples in order to evaluate the Young's modulus ( $E$ ) and to measure the elastic modulus of each cell. Sixty seconds was considered to be a reasonable resting period for the cells to achieve a new balance. At the end of each resting period, the aspirated length of the cell inside the needle was measured. Using a method of analysis applied in a previous study [3], the value of the Young's modulus was calculated from the slope of the applied pressure ( $\Delta p$ ). The normalized aspirated length of the cell ( $L/a$ ) was determined using the following equation, based on linear regression:

$$\Delta p = \frac{2\pi}{3} E \frac{L}{a} \varphi \quad (1)$$

where  $E$  is the Young's modulus of the cell,  $\Delta p$  and  $L$  represent the suction pressure and the aspirated length of the cell,  $a$  indicates the internal radius of the micropipette and  $\varphi$  describes the wall function. A typical value of  $\varphi$  is equal to 2.1, based on the punch model.

The cells were irradiated in the absorbed dose range of 0, 2, 4, 6, and 8 Gy. The response of the HUVECs to the application of stepwise suction pressure during micropipette aspiration was recorded to evaluate the elastic properties of a control cell (without an absorbed dose) (Fig. 2(a)) and in an irradiated cell (a dose of 8 Gy) (Fig. 2(b)).

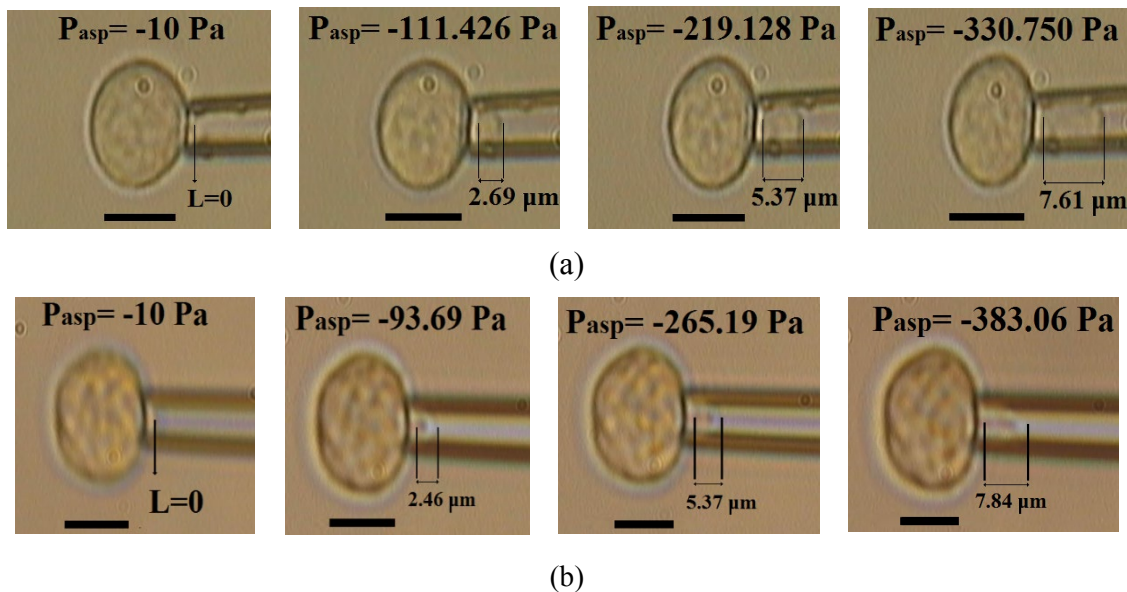


**Figure 2:** The response of a human umbilical vein endothelial cell to the application of stepwise suction pressure in micropipette aspiration to determine the elastic properties of individual cell for a) a control cell without an absorbed dose and b) an irradiated cell. The cell was irradiated at an absorbed dose of 2 Gy. The scale bar indicates 10  $\mu m$

The linear regression function and correlation of the coefficient between the suction pressure (Pa) and normalized aspiration length (L/a) was calculated for the control group and the exposed HUVECs (at absorbed doses of 2, 4, 6, and 8 Gy). The Young's modulus was calculated from the slope of the applied pressure ( $\Delta p$ ). The normalized aspirated length of the cell (L/a) was based on the linear regression function before and after irradiation with 0-8 Gy absorbed doses in 2 Gy steps. The dose-response curve for the Young's modulus for the range of absorbed doses was the plotted.

In living cells, compliance refers to the ability of a cell membrane to distend and increase its volume with increasing pressure, thereby resisting a return to its original dimensions on the application of a distending or compressing force [4,5]. The compliance of the single cells (C) was calculated from the induced maximal pressure [ $\Delta p$ (kPa)] and displacement of the cell membrane [L( $\mu\text{m}$ )] using the following equation [34]:

$$C = \frac{L}{\Delta p} \tag{2}$$

In this study, compliance parameter was calculated to compare the capacity of radiation-induced HUVECs at different radiation doses for cytoskeletal reorganization.

For assessing of creep response of a cell, we employ a generalized model of Maxwell model consist of a spring ( $k_1$ ) that provides the restoring force necessary to recover the initial shape after the release of the stress, arranged in parallel with another spring ( $k_2$ ) in series with an apparent viscosity ( $\mu$ ). To determine the creep behavior of each HUVEC, a constant critical pressure ranging in 205-500 Pa was applied to aspirate the cell and the aspiration trend was recorded for ranged in 140-280 s. In the following, the Creep compliance ( $J(t) = \frac{\text{aspiration length as a function of time}}{\Delta p}$ ) was extracted from the following equation [20,32]:

$$J(t) = \frac{1}{k_1} \left( 1 - e^{-\frac{t}{\tau}} \right) + \frac{e^{-\frac{t}{\tau}}}{k_1 + k_2} \tag{3}$$

where  $\tau$  is the time constant of the creep behavior.  $k_1$  and  $k_2$  are as the non-linear elastic coefficients are related to the equilibrium and instantaneous characteristics of cell stiffening, respectively. The procedure of assessing the spring constants  $k_1$  and  $k_2$  is to fitting a proper curve ( $f(x)=a.e^{-b.x+c}$ ) to the time-dependent length of cells creep into the micropipette based on the previous publications [31,32].

For assessing the elastic modulus of radiation-induced HUVECs, the sample size for each experiment group was  $N = 8$ . Also, assessing the Young's modulus of cells, the sample size for each experiment group was  $N = 5$ . Each experiment was performed at least five times and the resultant parameters were presented as the mean  $\pm$  standard deviation (SD). The Pearson correlation coefficient ( $r$ ) and linear regression function were calculated in relation to applied sequential pressure (Pa) and normalized aspiration length. A  $p < 0.050$  was considered to be statistically significant. Analysis of variance (ANOVA) analysis was carried out to compare the results obtained for the control group and for each irradiation-induced sample, given that a  $p < 0.050$  was considered to be statistically significant. All of the statistical analysis was performed using SPSS® software version 16.

### 3 Results

All of the individual cells exhibited a linear increase in aspiration length in response to the stepwise MA pressure-exerting process that was applied to evaluate cell elasticity (Pearson's correlation coefficient of  $> 0.98$ ). The elastic behavior of the HUVECs in the different treatment groups was determined (Fig. 3).

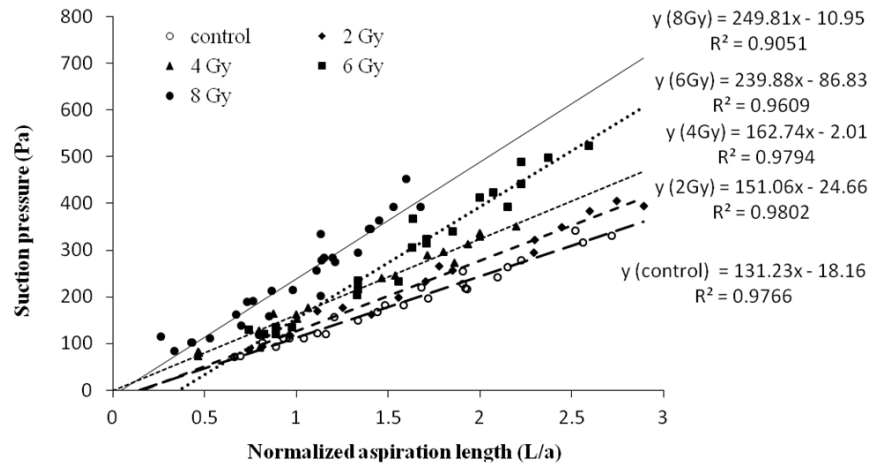


**Figure 3:** A depiction of the elastic behavior of human umbilical vein endothelial cells exposed to different ionizing radiation doses. The effective Young’s modulus of each group is indicated by the relevant line pertaining to the slope

The linear regression function and correlation of the coefficients with suction pressure (Pa) and normalized aspiration length (L/a) were determined for the control group and exposed HUVECs (at absorbed doses of 2, 4, 6, and 8 Gy) (Fig. 4) ( $p < 0.05$ ). The results show that with each increase in the absorbed dose, the slope of the curve from 0-8 Gy correspondingly increased when compared to the control group (15%, 24%, 83%, and 90%, respectively).

The Young’s modulus of the HUVECs increased along with the increase in the absorbed dose. Values of  $29.87 \pm 1.04$  Pa,  $34.99 \pm 0.85$  Pa,  $37.30 \pm 0.95$  Pa,  $55.82 \pm 1.44$  Pa, and  $57.99 \pm 1.76$  Pa were reported for the absorbed doses of 0, 2, 4, 6, and 8 Gy, respectively. The difference in the Young’s modulus of the cells with each increase in the absorbed dose was statistically significant ( $p < 0.01$ ). Significant differences between the Young’s modulus (Pa) of the exposed HUVECs (at absorbed doses of 0, 2, 4, 6, and 8 Gy) ( $p < 0.05$ ) was demonstrated using Fisher’s least significant difference test. The dose-response curve for Young’s modulus (Pa) of the absorbed doses (0-8 Gy) in 2 Gy steps was calculated (Fig. 4).

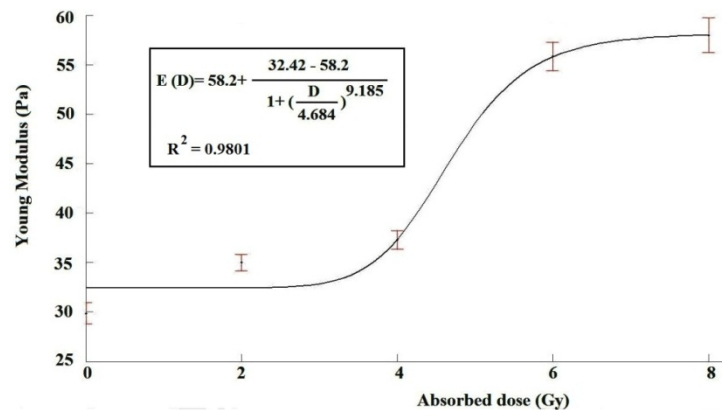


**Figure 4:** The dose-response curve for Young’s modulus (Pa) of the absorbed doses (0-8 Gy) in 2 Gy steps was calculated for human umbilical vein endothelial cells. E(D) represents a fitted curve of elastic curve behavior as a function of absorbed doses

In the current study, a fourth-order sigmoidal curve was fitted to the dose response using the previously mentioned dose value range (0, 2, 4, 6, and 8 Gy). The coefficient variation for the parameters at any dose was less than 4%. Following analysis of the linear portion of the response curve (Fig. 4), the

correlation coefficient for the linear range of the curve was found to be 0.955 and the sensitivity of Young’s modulus curve in relation to the doses was 7.69 Pa..Gy-1.

The compliance (kPa/μm) properties of the endothelial cells in response to the radiation therapy doses is shown in Tab. 1. A considerable downward shift in the compliance curve, when compared to that for the control group, was demonstrated in relation to the HUVECs irradiated by ionizing photons. A significant fall in the level of compliance was also observed after completion of the ionizing radiation (Tab. 1).

**Table 1:** Compliance parameter of endothelial cells irradiated to single ionizing radiation doses

	Control	2 Gy	4 Gy	6 Gy	8 Gy	<i>p</i> -value *
<i>Compliance</i> (μm/Pa)	62.88 ± 17.32	43.17 ± 1.06	45.00 ± 1.16	27.44 ± 0.70	37.43 ± 16.14	0.001

A *p*-value of 0.05 describes significant change in results in ANOVA.

These results correlated with the elastic behavior of the radiation-induced cells. It is clear that all of the aforementioned parameters for HUVECs irradiated by ionizing photons were significantly different from those in the baseline group. However, the decrease in compliance observed between the samples irradiated by 2 Gy and those irradiated with the 4, 6, and 8 Gy doses was not statistically significant. In addition, the compliance of cells irradiated by 6 Gy was not significantly different from those exposed to the 8 Gy radiation dose (*p* > 0.05). However, compliance, as a parameter, was not seen as one that could approach statistical significance in this study.

In order to evaluation of the viscoelastic behavior, upon applying specific suction pressure on HUVECs through the micropipette, aspirated length into the needle exhibited immediate jump and then the aspiration rate uniformly decreased and finally stabilized its balance length. In the micropipette aspiration tests, all of the HUVECs display a typical monotonic viscoelastic behavior and the correlation coefficients of R2 > 0.95 were revealed. Our experimental data exhibited that the normalized aspiration length (L/a) for non-irradiated samples is greater than 4. In contrary, values of this parameter in irradiated HUVECs are obviously less than that in control cells (i.e., L/a ratio values for HUVECs irradiated by 8 Gy radiation dose are < 3). Also, the mean value of time constant parameter in non-irradiated group is 2.5 times more than that of radiation-induced cells. While, the time constant did not show any significant change during treatment by different ionizing doses. The necessary time to achieve the equilibrium aspiration length for non-irradiated and radiation-induced HUVECs is about 150 and 50 s, respectively.

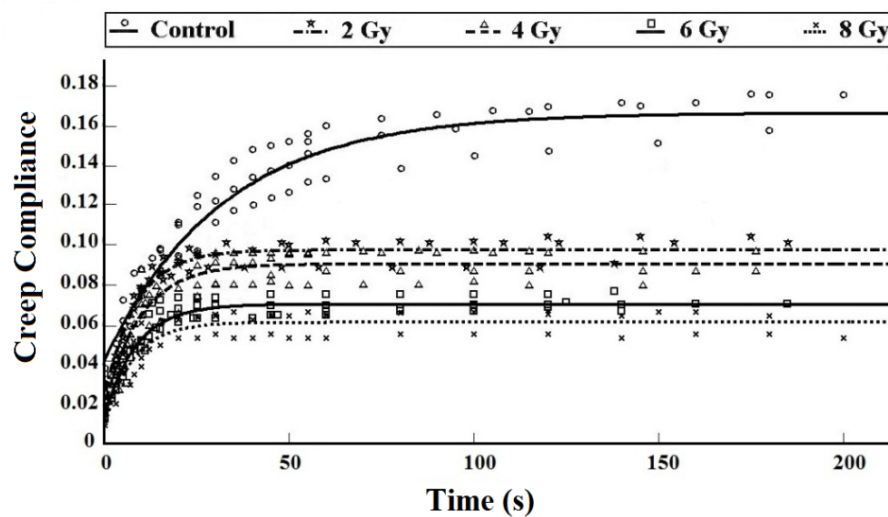


**Figure 5:** Alteration in creep compliance curves of HUVECs exposed to different ionizing radiation doses

As shown in Fig. 5, HUVECs irradiated by ionizing photons have a considerable downward shift in creep compliance curve compared to the baseline group. These outcomes correlated with elastic behavior of radiation-induced cells.

The actin cytoskeleton of the HUVECs was analyzed using confocal imaging of each group (Fig. 6).

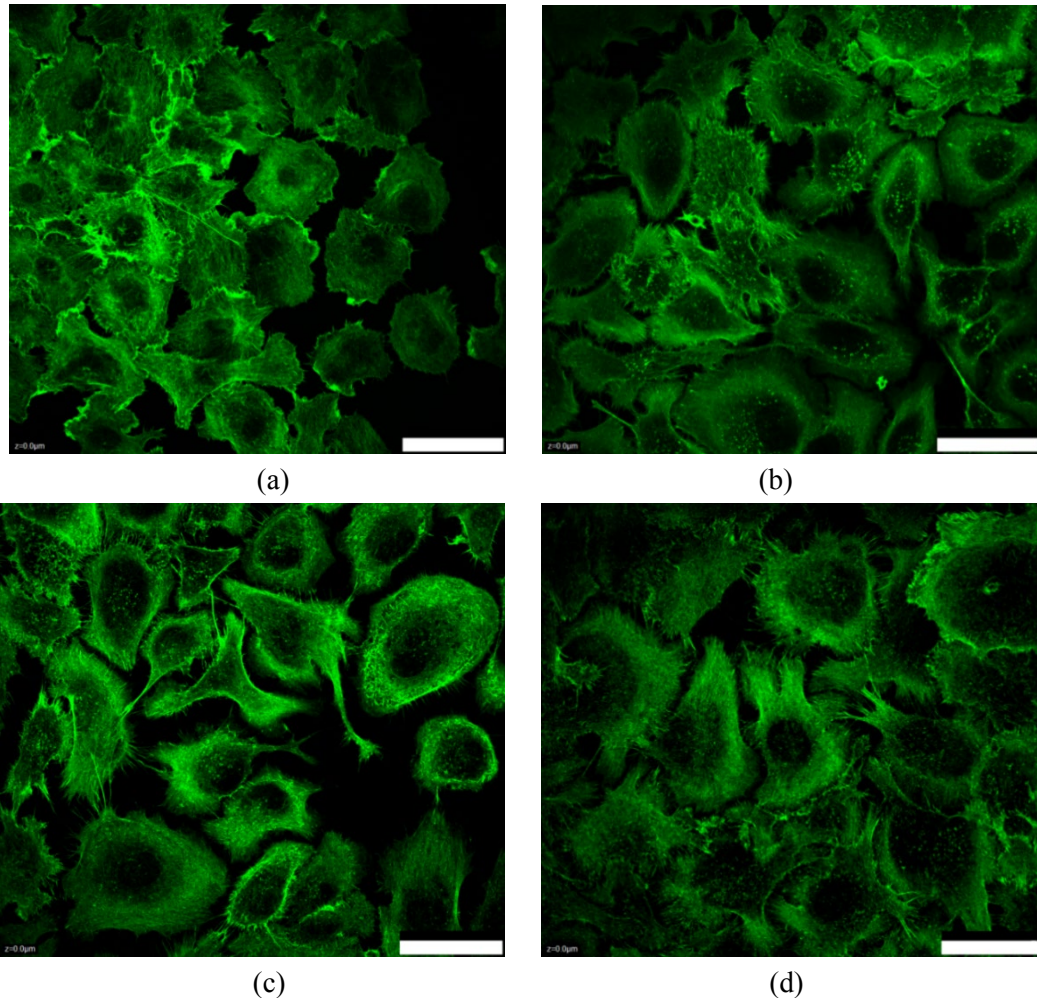


**Figure 6:** The absorbed doses caused the formation of actin filament remodeling in the human umbilical vein endothelial cells. The cells were irradiated with a) 0 Gy, b) 2 Gy, c) 4 Gy and d) 8 Gy, fixed within 24 hours of irradiation and stained for F-actins. The scale bars indicate 50  $\mu\text{m}$

As cytoskeletal changes are known to be a biomarker of change to the mechanical properties of cells, the influence of ionizing radiation doses on the HUVEC cytoskeleton was analyzed, in conjunction with the use of MA. It is likely that the accumulation of stress fibers in the cortex occurred in response to ionizing irradiation in HUVECs. Moreover, an increase in the size of the nuclei in the radiated HUVECs was observed to be accompanied by the cell stiffening (Fig. 7).



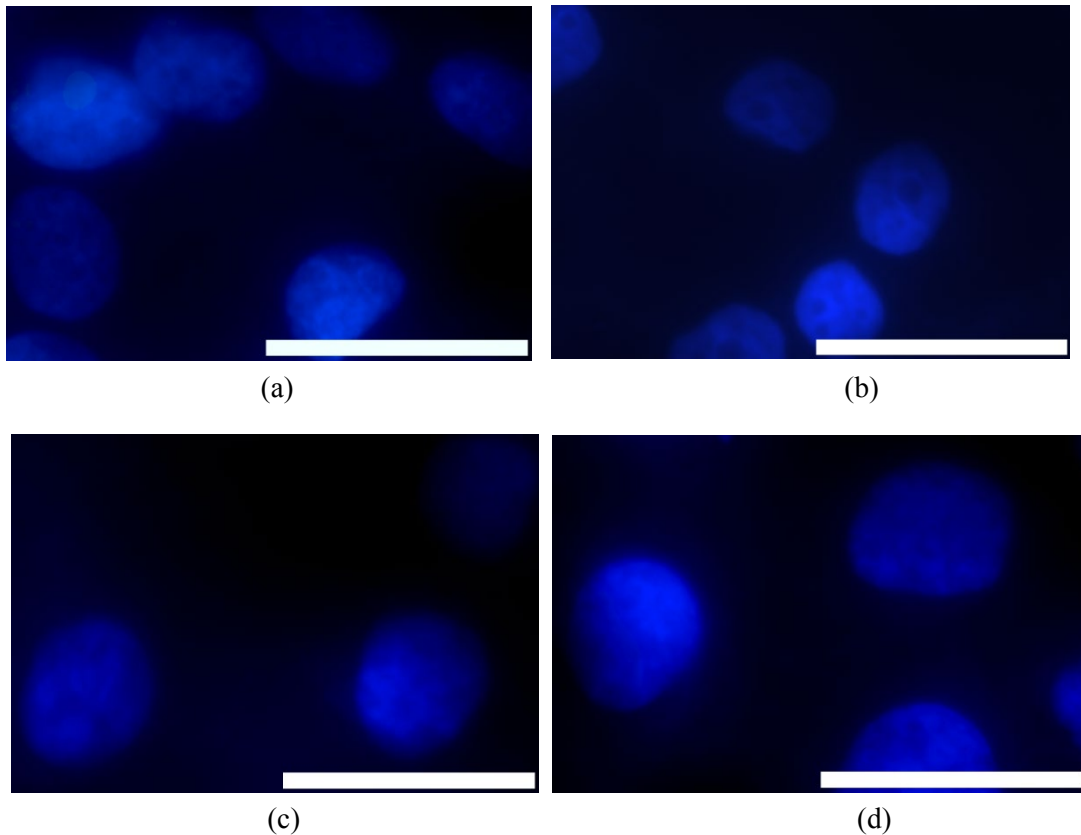


**Figure 7:** An increase in the ionizing radiation dose value led to a corresponding increase in the nuclei size of the human umbilical vein endothelial cells. The cells were irradiated with a) 0 Gy, b) 2 Gy, c) 4 Gy and d) 8 Gy, fixed within 24 hours of irradiation and stained for cell nucleus. The scale bars indicate 50  $\mu\text{m}$

The area of HUVECs in 0, 2, 4 and 8 Gy treatment situations were obtained as  $1290.15 \pm 282.81 \mu\text{m}^2$ ,  $1728.93 \pm 1024.14 \mu\text{m}^2$ ,  $1567.42 \pm 914.01 \mu\text{m}^2$ , and  $2597.60 \pm 388.13 \mu\text{m}^2$ , respectively. Moreover, the area of HUVECs nuclei in 0, 2, 4 and 8 Gy treatment positions were obtained as  $188.87 \pm 49.69 \mu\text{m}^2$ ,  $217.22 \pm 25.71 \mu\text{m}^2$ ,  $256.90 \pm 32.33 \mu\text{m}^2$ , and  $348.71 \pm 38.14 \mu\text{m}^2$ , respectively. It is noteworthy that the increase in the ionizing radiation dose led to a corresponding increase in the size of the HUVECs. It seems that the increase in nuclei size was a consequence of the creation of disorder in the radiation-induced cells.

Moreover, the perimeter around the membrane and nuclei of each cell were measured to assess the cell shape index and nuclei shape index of HUVECs after radiotherapy process, respectively (Tab. 2). The findings illustrate that increasing the single irradiation dose from 0 to 8 Gy led to a significant decrease of cell shape index (approximately 56%) and a significant increase of nuclei shape index (approximately 85%). These changes can support the mechanism of cytoskeletal changes.

**Table 2:** Shape index parameters of whole body and nuclei of endothelial cells irradiated to single ionizing radiation doses

Shape index	Control	2 Gy	4 Gy	8 Gy	<i>p</i> -value *
<i>Membrane</i>	0.73 ± 0.06	0.60 ± 0.13	0.45 ± 0.13	0.32 ± 0.09	< 0.001
<i>Nuclei</i>	0.49 ± 0.14	0.88 ± 0.03	0.90 ± 0.03	0.91 ± 0.02	< 0.001

\*A *p*-value of 0.05 describes significant change in results in ANOVA.

#### 4 Discussions

Radiation therapy is usually considered to be an effective treatment for various types of cancers. However, ionizing irradiation results in adverse effects, such as cardiovascular disease, by damaging the monolayer cells of the endothelium surrounding the target area [9]. It has been reported that high doses of ionizing radiation (> 8 Gy) cause substantial damage to the endothelial cell membrane, significantly increasing the rate of cell death [17].

Thus, the mechanical behavior of HUVECs in control and irradiated samples (ionizing radiation doses up to 8 Gy) as evaluated in the current study. The trend of elastic behavior in radiation-induced endothelial cells follows the sigmoidal curve and is similar to a basic radiobiological dose response.

Our results indicate that ionizing radiation did not perceptibly alter the cytoskeletal structure of the HUVECs immediately after exposure (unpublished data). These findings are confirmed by those in a previous published study in which the radiation effects on the cytoskeleton of the endothelial cells were investigated. It was found that radiation caused the rapid formation of stress fibers in the dermal microvascular endothelial cells, but not in the HUVECs [16]. We observed that with the passing of an adequate length of time, following the exposure of cells to radiation, the cytoskeletal microfilament of the HUVECs underwent considerable changes in terms of their organization. Confocal images (Fig. 6) illustrated that 24 hours after ionization, the number of F-actin fibers increased in comparison with that in the untreated samples. In addition, there was a reduction in fiber length. Moreover, HUVECs lose the circular shape by increasing the absorbed dose and turn into linear shape (Tab. 2).

We observed that the increase in the nuclei size in the HUVECs was affected by ionizing radiation 24 hours after exposure (Fig. 7). In addition, nuclei of radiation-induced HUVECs turn into a circular form (Tab. 2). This is a consequence of DNA damages such as double-strand breaks [19]. Similar changes in the size of the nuclei (of 5 Gy) in the radiation-induced HUVECs were reported in another study [2]. An increase in the size of the nuclei in the radiated HUVECs was correspondingly accompanied by a decrease in the cortex thickness in the cells (Fig. 7). Thus, the probability of a cross-link formation between the fibers increased. It is well-known that cytoskeletal remodeling has an influence on the mechanical behavior of cells. Accordingly, anticipated changes were found with respect to the mechanical properties of the radiation-induced HUVECs, through cell stiffening (evidenced by a significantly enhanced Young's modulus) and a decrease in the compliance parameter, when compared to that reported for the untreated samples (Tab. 1).

Interestingly, the ionizing radiation doses induced appreciable differences in the localization of the F-actins and cytoskeleton proteins, i.e., in the tight junction-associated proteins (VE-cadherin) and platelet endothelial cell adhesion molecules [1]. In addition, the expression of vascular cell adhesion molecule 1 gene was found to be remarkably decreased in the radiation-exposed HUVECs [9]. Moreover, the expression levels of several genes are remarkably increased in radiation-induced endothelial cells as reported in previous study [1]. It has been proved that the genetic changes induce signals that reorganized the cytoskeleton [14]. An increment in endothelial cell permeability, in response to ionizing photon irradiation, was reported 24 hours after dissipation of the ionizing dose [1,13,19]. An interesting outcome of the present study was changes to the adhesion and permeability of the radiation-induced endothelial cells, also reported in previous studies, and considered to be a sign of vascular damage. The consequences of this were cytoskeletal changes, along with an obvious variation in the mechanical behavior of the cells,

when compared with corresponding parameters in the control group.

## 5 Conclusion

It is concluded that because of endothelial properties variations after single dose radiation therapy, the vascular injuries was occurred in the long term. In the other word, endothelial cells are suggested as the regulators of extracellular matrix in response to ionizing radiation and changes of their mechanical properties will lead to vascular damages such as lumen stenosis and atherosclerosis. This study illustrated that cancer treatment using gamma irradiation leads to a significant change in mechanical behavior of vascular endothelial cells. Therefore, we suggest that the function of main vessels for patients that receives radiation therapy doses will have been considered more than ever by oncologists and radiotherapists. It was established in the current study that long-term vascular injuries resulted from variations to the endothelial properties following radiation therapy. This suggests that the endothelial cells are regulators of the extracellular matrix in response to ionizing radiation and that changes to their mechanical properties lead to vascular damage, such as lumen stenosis and atherosclerosis.

It was illustrated in this study that cancer treatment with gamma irradiation led to a significant change in the mechanical behavior of the vascular endothelial cells. Therefore, it is suggested that the function of the major blood vessels in patients receiving radiation therapy needs to be further investigated by oncologists and radiotherapists in future studies.

**Acknowledgment:** This study was approved by Tarbiat Modares University. This work was supported in part by the Iran National Science Foundation (INSF).

**Conflicts of Interest:** None declared.

## References

1. Sharma P, Templin T, Grabham P. Short term effects of gamma radiation on endothelial barrier function: Uncoupling of PECAM-1. *Microvascular Research* **2013**, 86: 11-20.
2. Rombouts C, Aerts A, Beck M, Vos WHD, Oostveldt PV et al. Differential response to acute low dose radiation in primary and immortalized endothelial cells. *International Journal of Radiation Biology* **2013**, 89: 841-850.
3. Theret DP, Levesque MJ, Sato M, Nerem RM, Wheeler LT. The application of a homogeneous half-space model in the analysis of endothelial cell micropipette measurements. *Journal of Biomechanical Engineering* **1998**, 110: 190-199.
4. Sato M, Theret DP, Wheeler LT, Ohshima N, Nerem RM. Application of micropipette technique to measurement of cultured porcine aortic endothelial cell viscoelastic properties. *Journal of Biomechanical Engineering* **1990**, 112: 263-268.
5. Sato M, Ohshima N, Nerem RM. Viscoelastic properties of cultured porcine aortic endothelial cells exposed to shear stress. *Journal of Biomechanics* **1996**, 29: 461-467.
6. Hatami J, Tafazzoli-Shadpour M, Haghypour N, Shokrgozar MA, Janmaleki M. Influence of cyclic stretch on mechanical properties of endothelial cells. *Experimental Mechanic* **2013**, 53: 1291-1298.
7. Bischof M, Abdollahi A, Gong P, Stoffregen C, Lipson KE et al. Triple combination of irradiation, chemotherapy (pemetrexed), and VEGFR2 in human endothelial and tumor cells. *International Journal Radiation Oncology Biology Physics* **2004**, 60: 1220-1232.
8. Samandari MM, Abrinia K, Mokhtari-Dizaji M, Tamayol A. Ultrasound induced strain cytoskeleton rearrangement: an experimental and simulation study. *Journal of Biomechanics* **2017**, 60: 39-47.
9. Jelonek K, Walaszczyk A, Gabrys D, Pietrowska M, Kanthou CC et al. Cardiac endothelial cells isolated from mouse heart-a novel model for radiobiology. *Acta Biochimica Polonica* **2011**, 58: 397-404.
10. Cheng SWK, Ting ACW, Wu LLH. Ultrasonic analysis of plaque characteristics and intimal-medial thickness in radiation-induced atherosclerotic carotid arteries. *European Journal of Vascular and Endovascular Surgery*

- 2002**, 24: 499-504.
11. Garcez K, Lim CC, Whitehurst P, Thomson D, Ho KF et al. Carotid dosimetry for T1 glottic cancer radiotherapy. *British Journal Radiology* **1998**, 87: 1-8.
  12. McDonald MW, Moore MG, Johnstone PAS. Risk of carotid blowout after reirradiation of the head and neck: a systematic review. *International Journal of Radiation Oncology, Biology, Physics* **2012**, 82: 1083-1089.
  13. Gujral DM, Shah BN, Chahal NS, Senior R, Harrington KJ et al. Clinical features of radiation-induced carotid atherosclerosis. *Clinical Oncology* **2014**, 26: 94-102.
  14. Yu H, Tay CY, Leong WS, Tan SCW, Liao K et al. Mechanical behavior of human mesenchymal stem cells during adipogenic and osteogenic differentiation. *Biochemical and Biophysical Research Communications* **2010**, 393: 150-155.
  15. Assis MC, Plotkowski MC, Fierro IM, Barja-Fidalgo C, de Freitas MS. Expression of inducible nitric oxide synthase in human umbilical vein endothelial cells during primary culture. *Nitric Oxide* **2002**, 7: 254-261.
  16. Gabrys D, Greco O, Patel G, Prise KM, Tozer GM et al. Radiation effects on the cytoskeleton of endothelial cells and endothelial monolayer permeability. *International Journal Radiation Oncology Biology Physics* **2007**, 69: 1553-1562.
  17. Kaffas AE, Al-Mahrouki A, Tran WT, Giles A, Czarnota GJ. Sunitinib effects on the radiation response of endothelial and breast tumor cells. *Microvascular Research* **2014**, 92: 1-9.
  18. Kern PM, Keilholz L, Forster C, Hallmann R, Herrmann M et al. Low-dose radiotherapy selectively reduces adhesion of peripheral blood mononuclear cells to endothelium *in vitro*. *Radiotherapy and Oncology* **2000**, 54: 273-282.
  19. Kim KS, Kim JE, Choi KJ, Bae S, Kim DH. Characterization of DNA damaged-induced cellular senescence by ionizing radiation in endothelial cells. *International Journal of Radiation Biology* **2014**, 90: 71-80.
  20. Mohammadkarim A, Tabatabaei M, Parandakh A, Mokhtari-Dizaji M, Tafazzoli-Shadpour M et al. Radiation therapy affects the mechanical behavior of human umbilical vein endothelial cells. *Journal of the Mechanical Behavior of Biomedical Materials* **2018**, 85: 188-193.
  21. Mohammadkarim A, Mokhtari-Dizaji M, Kazemian A, Saberi H, Khani MM et al. Dose-dependent <sup>60</sup>Co  $\gamma$ -radiation effects on human endothelial cell mechanical properties. *Cell Biochemistry and Biophysics* **2019**, 77: 179-186.
  22. Khan FM, Gibbons JP. *The Physics of Radiation Therapy*, Fifth Edition, pp. 102-111. Baltimore: William and Wilkins. **2014**.
  23. Zheng Q, Liu Y, Zhou HJ, Du YT, Zhang BP et al. X-ray radiation promotes the metastatic potential of tongue squamous cell carcinoma cells via modulation of biomechanical and cytoskeletal properties. *Human and Experimental Toxicology* **2015**, 34: 894-903.
  24. Aryaei A, Jayasuriya AC. Mechanical properties of human amniotic fluid stem cells using nanoindentation. *Journal Biomechanics* **2013**, 46: 1524-1530.
  25. Goldmann WH, Galneder R, Ludwig M, Kromm A, Ezzell RM. Differences in F9 and 5.51 cell elasticity determined by cell poking and atomic force microscopy. *FEBS Letters* **1998**, 424: 139-142.
  26. Guo Q, Xia Y, Sandig M, Yang J. Characterization of cell elasticity correlated with cell morphology by atomic force microscope. *Journal of Biomechanics* **2012**, 45: 304-309.
  27. Li OS, Lee GYH, Ong CN, Lim CT. AFM indentation study of breast cancer cells. *Biochemical and Biophysical Research Communications* **2008**, 374: 609-613.
  28. Rebelo LM, Sousa JS, Filho JM, Radmacher M. Comparison of the viscoelastic properties of cells from different kidney cancer phenotypes measured with atomic force microscopy. *Nanotechnology* **2013**, 24: 1-12.
  29. Guilak F, Tedrow JR, Burgkart R. Viscoelastic properties of the cell nucleus. *Biochemical and Biophysical Research Communications* **2014**, 269: 781-786.
  30. Pachenari M, Seyedpour SM, Janmaleki M, Babazadeh SS, Taranejoo S et al. Mechanical properties of cancer cytoskeleton depend on actin filaments to microtubules content: Investigating different grades of colon cancer cell lines. *Journal of Biomechanics* **2014**, 47: 373-379.
  31. Seyedpour, S.M., Pachenari, M., Janmaleki, M., Alizadeh, M., Hosseinkhani, H. Effects of an antimetabolic drug on mechanical behavior of the cytoskeleton in distinct grades of colon cancer cells. *Journal of Biomechanics*

- 2015**, 48: 1172-1178.
32. Khani M, Tafazzoli-Shadpour M, Goli-Mlekabadi Z, Haghypour N. Mechanical characterization of human mesenchymal stem cells subjected to cyclic uniaxial strain and TGF- $\beta$ 1. *Journal of the Mechanical Behavior of Biomedical Materials* **2015**, 43: 18-25.
  33. Thakar RG, Ho F, Huang NF, Liepmann D, Li S. Regulation of vascular smooth muscle cells by micropatterning. *Biochemical and Biophysical Research Communications* **2003**, 307: 883-890
  34. Potter CMF, Schobesberger S, Lundberg MH, Weinberg PD, Mitchell JA et al. Shape and compliance of endothelial cells after shear stress in vitro or from different aortic regions: scanning ion conductance microscopy. *Study PLoS One* **2012**, 7: e31228.